HHS Public Access

Author manuscript

Anal Chim Acta. Author manuscript; available in PMC 2020 September 23.

Published in final edited form as:

Anal Chim Acta. 2019 September 23; 1072: 75–80. doi:10.1016/j.aca.2019.05.001.

Nicking Enzyme-Assisted Signal-Amplifiable Hg^{2+} Detection Using Upconversion Nanoparticles

Anjaly N. Vijayan[1], **Zhiming Liu**[2], **Haohan Zhao**[1], and **Peng Zhang**[1]

[1]Department of Chemistry, University of Cincinnati, OH 45221, USA

[2]National Engineering Laboratory for Green Chemical Productions of Alcohols, Ethers and Esters, College of Chemistry & Chemical Engineering, Xiamen University, Xiamen 361005, China

Abstract

A highly specific and sensitive isothermal method for mercury detection using DNA-conjugated upconversion nanoparticles is reported. A single-stranded DNA containing thymine bases, used as the Hg^{2+}-capturing element utilizing the bond formation of Thymine-Hg^{2+}-Thymine complex, is covalently attached to the $NaYF_4$: Yb^{3+}, Tm^{3+} nanoparticles. Luminescence resonance energy transfer takes place between the NaYF4: Yb^{3+}, Tm^{3+} nanoparticles as donor and DNA-intercalating SYBR Green I as the acceptor upon excitation of 980 nm. The sensitivity and selectivity toward Hg^{2+} are enhanced using the nicking enzyme, Nt. Alwl, which leads to signal amplification. By monitoring the ratio of acceptor emission to a reference peak, the presence of Hg^{2+} ions are quantitatively determined with a lower detection limit of 0.14 nM, which is much lower than the US Environmental Protection Agency (EPA) limit of Hg^{2+} in drinking water.

Graphical Abstract

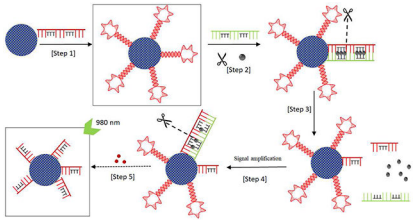

We report a highly specific and sensitive isothermal method for Hg^{2+} ion detection using DNA-conjugated upconversion nanoparticles.

Declaration of interests

☒ The authors declare that they have no known competing financial interests or personal relationships that could have appeared to influence the work reported in this paper.

Keywords

Upconversion nanoparticles (UCNPs); mercuric ion; luminescence resonance energy transfer (LRET); nicking enzyme; signal amplification

1. Introduction

According to World Health Organization (WHO), solvated mercuric ion (Hg^{2+}), one of the most stable inorganic forms of mercury, is considered as one of the top chemicals of major public health concern. It is a caustic and carcinogenic species with high cellular toxicity[1–3]. Mercuric ion is highly harmful even at low concentrations and can be transformed by microbial methylation into methylmercury, which leads to serious and permanent damage to the brain with acute toxicity [4,5]. Because of its chemical stability with relatively long residence time ranging from months to years, the routine detection of Hg^{2+} is crucial in the monitoring of larger bodies of water and the safety evaluation of aquatically derived food supplies [6].

Conventional mercury detection techniques include atomic absorption/emission spectroscopy and inductively coupled plasma mass spectroscopy (ICPMS). Even though these techniques achieve very low detection limit (<0.9 nM), they involve sophisticated instruments and laborious procedures. Several methods for the detection of mercury has been reported [7] using colorimetric [7–11], electrochemical [12–15], fluorescence techniques [16–19], etc. Nanoparticles such as gold nanoparticles [8, 9, 11, 20], carbon nanotubes [21], graphene oxide [22], and quantum dots [19], have been used in the detection of mercuric ions in aqueous solutions. Since the maximum allowable level of mercuric ion in drinkable water set by US Environmental Protection Agency [23] is 10 nM, there is an ongoing demand for the development of detection methods that are sensitive, specific, and easy to use.

In recent years, there has been a growing interest in developing upconversion nanoparticles (UCNPs) that can emit higher energy photons after absorbing lower energy photons. Sharp emission lines, long luminescence lifetimes, superior photostability, and absence of autofluorescence resulting in high signal-to-noise ratio are the unique features of UCNPs. There are reports where UCNPs in combination with fluorescent dyes are used for detecting nucleotides [24–27]. Mercuric ions can be selectively determined using DNA sequences. Several mercury forms, both inorganic and organic types, can bind to DNA and result in conformational changes in the DNA structure [28–31]. There are also reports where Thymine-Thymine pair in DNA strands are used to specifically detect mercuric ion [8],[32]–[33]. In this report, a novel signal-amplification method with good specificity and selectivity is shown to detect Hg^{2+} ions in aqueous media using nicking enzyme under isothermal conditions, based on the energy transfer between UCNPs and the DNA-intercalating dye, SYBR Green I.

2. Materials and Methods

2.1. Chemicals and materials

All chemicals were used as received without further purification. Sodium chloride (NaCl), yttrium nitrate ($Y(NO_3)_3{\cdot}6H_2O$), ytterbium nitrate ($Yb(NO_3)_3{\cdot}5H_2O$), thulium nitrate ($Tm(NO_3)_3$-$5H_2O$), , ammonium fluoride (NH_4F), polyacrylic acid (PAA, MW ~15000), polyacrylic acid (PAA, MW ~1800), barium carbonate ($BaCO_3$), cupric chloride ($CuCl_2$), cobalt chloride ($CoCl_2$), zinc sulfate ($ZnSO_4$), and mercury(II) nitrate monohydrate ($Hg(NO_3)_2{\cdot}H_2O$) were purchased from Sigma Aldrich (St. Louis, MO). 1-Ethyl-3-[3-dimethylamonopropyl] carbodiimide hydrochloride (EDC), *N*-hydroxysuccinimide (NHS) and ethylene glycol (EG) were purchased from Thermo Scientific (Rockford, IL). SYBR Green I was from Life Technology (Carlsbad, CA). All DNA strands were from IDT DNA (Coralville, IA). Nt. Alwl and 10x Cutsmart® buffer were purchased from New England BioLabs. The melting points of various DNA strands under the experimental conditions were estimated using the OligoAnalyzer program available at the vendor's website (http://www.idtdna.com). The sequences of DNA probes used in this study are listed in Table 1. The DNA strands used are DNA_1 (22mer, amine-modified at the 5'-end) and DNA_mismatch (22mer). The middle segment of DNA_mismatch is complementary to DNA_1 except at the thymine bases.

2.2. Synthesis of $NaYF_4$; Yb^{3+}, Tm^{3+} upconversion nanoparticles

PAA (MW ~ 15 000, 1.950 g), PAA (MW ~1800, 0.645 g), NaCl (0.203 g), Y(NO3)3'$6H_2O$ (0.527 g), $Yb(NO_3)_3{\cdot}5H_2O$ (0.151 g), and $Tm(NO_3)_3{\cdot}5H_2O$ (0.003 g) were mixed into 26 mL of EG, using vortex and sonicator to form a homogenous mixture (Solution A). Separately, 0.24 g of NH_4F was dispersed into 16 mL of EG in a Teflon container (Solution B). Solution A was added into Solution B drop wise under vigorous stirring for 1 hour. The Teflon container was then placed in a sealed stainless-steel capsule and heated in an oven at 220 °C for 24 h. The resulting solution obtained was clear with light brown in color. The nanoparticles were collected by centrifugation at 48,000 rpm for 1 h to remove the supernatant. Pellet was washed 3 times by ethanol and twice by DI water before storing for later use.

2.3. Conjugation of DNA_1 to UCNPs

Two mL of UCNP aqueous solution was treated with 10 μL of 0.2 M EDC and 10 μL of 0.05 M NHS for 15 min under stirring at 600 rpm in an ice bath. Next, 10 μL of 1 mM DNA_1 was added into the mixture and stirred at 600 rpm overnight. The resulting nanoparticles were washed 3 times by DI water, before dispersed in 1 mL of DI water.

2.4. Determination of conjugation yield of DNA_1 to UCNPs

The amount of DNA_1 conjugated to the UCNPs was determined experimentally. A standardization curve of DNA_1 with SYBR Green I solution was first obtained using DNA_1 solutions of different concentrations (0, 10, 20, 30, 40, 50, 70 nM). In these measurements, SYBR Green I was excited at 480 nm using a Xenon lamp with 1-mm slit width, and the emission intensity at 520-540 nm was measured. Then DNA_1-conjugated

UCNP working solution (UCNP-DNA_1) was incubated with the same amount of SYBR Green I solution and excited at 480 nm. The concentration of DNA_1 in the DNA_1-conjugated UCNP solution was calculated based on the standardization curve.

2.5. DNA nicking and mercuric ion sensing

DNA_1 conjugated UCNP solution (30 μL) was added into 10x Cutsmart® buffer (39 μL) and DNA_mismatch (30 μL). The mixture was brought to a total volume of 390 μL using DI H_2O, and treated in 90 °C for 5 min. The solution was cooled down to 37 °C (optimal temperature for Nt. Alwl) and maintained for 3 min before adding Nt. Alwl (20 units). Different concentration of Hg^{2+} (0, 0.2, 0.5, 1.0, 1.5, 2.0 nM) was then added to the vial containing DNA_mismatch. The solution was kept at 37 °C for 2 h in a thermal cycler, before being heated again to 90 °C to deactivate the nicking enzyme.

2.6. Luminescence measurements under 980 nm excitation

The UCNP-DNA_1 mixture after the thermal treatment was mixed with 2 μT of 10x SYBR Green I solution and transferred into a quartz cuvette. Emission spectra were collected on a spectrofluorometer (PTI) equipped with an external 980-nm laser (Laserglow Technology, Canada) as the excitation source. Slit width was set at 1.0 mm. When calculating the ratio of I_{477}/I_{800}, I_{477} refers to the integrated area between 468 to 490 nm and I_{800} to that between 770 to 830 nm. All measurements were done in triplicates.

2.7. Specificity and complex matrix studies

Different concentrations of Cu^{2+}, Co^{2+}, Zn^{2+}, Ba^{2+} in DI water (0.2, 1.0, 2.0 nM) were tested with the same procedure as described above. Tap water was collected and known concentrations of Hg^{2+} were spiked to the sample (0.5, 1.4 nM). This water sample was tested using the proposed detection method. The lake water was collected from Burnet Woods Lake, Cincinnati. It was centrifuged for 30 minutes at 10,000 rpm and the supernatant was collected. The concentration of Hg^{2+} was detected by ICPMS. Proper dilutions were made to make the concentration fall in the range of the calibration curve. The diluted samples were tested with the above procedure and the luminescence spectra were recorded. All measurements were taken in triplicates.

3. Results and Discussion

Yb^{3+}/Tm^{3+} co-doped $NaYF_4$ UCNPs used in this study are synthesized by a previously reported hydrothermal method [34] and are well dispersed in water. The particles synthesized by this method have carboxylic acid groups present on the surface, which not only render the hydrophilicity but also facilitate further functionalization. Transmission electron microscopy (TEM) image of UCNPs is shown in Figure 1. It shows hexagonal UCNPs with a diameter of 188 ± 14 nm. Photoluminescence spectrum of the UCNPs is also shown in Figure 1. Upconversion of the synthesized particles can be visualized by naked eyes when excited with a 980-nm laser.

DNA_1, a 22-mer modified with $-NH_2$ group at its 5’ end, is covalently conjugated to the UCNPs through the widely used EDC/NHS method. SYBR Green I, a DNA intercalating

dye, was used to quantify the amount of DNA_1 on the surface of the UCNPs. Upon excitation with 480 nm, SYBR Green I, emits weak fluorescence when it binds to single stranded DNA. Upon binding to double-stranded DNAs, the fluorescence of SYBR Green I is enhanced by ~1000-fold [35]. The standardization curve of DNA_1 in 0.5 μM SYBR Green I solution was established with different concentrations of DNA_1 (Figure 2), which showed a linear relationship between the fluorescence intensity of SYBR Green I and the DNA_1 concentration (Figure 2). Fluorescence spectra were collected for SYBR Green I with UCNPs before and after conjugated with DNA_1 under 480 nm excitation. The DNA_1 concentration in the UCNP-DNA_1 stock solution was determined to be 47nM.

The detection scheme is illustrated in Figure 3. DNA_1 is first conjugated to the UCNP surface, forming UCNP-DNA_1. Five nucleotides on both the ends of DNA_1 are complementary to each other, facilitating the formation of a hairpin loop with a melting temperature of ~51 °C under the assay conditions. DNA_mismatch itself would also form a hairpin loop with a melting temperature of ~37 °C. The sequence of DNA_mismatch is mostly complementary to DNA_1 except for the six thymine bases highlighted in bold red in the sequence (Table 1). In the absence of Hg^{2+}, DNA_1 and DNA_mismatch will form respective hairpin structures rather than binding to each other. In the presence of Hg^{2+}, DNA_1 and DNA_mismatch become completely complementary to each other, forming a dsDNA via Thymine-Hg^{2+}-Thymine (T-Hg^{2+}-T) chemistry. T-T mismatch displays excellent selectivity toward Hg^{2+} against many other metal ions [36], and has been widely used in the development of Hg^{2+} sensors. The melting temperature of the dsDNA of DNA_1 and DNA_mismatch (56 °C) is higher than those of individual hairpin structures of DNA_1 and DNA_mismatch, facilitating the formation of dsDNA over the individual hairpin structures of DNA_1 and DNA_mismatch. Note that, in the presence of Hg^{2+}, the dsDNA formed between DNA_1 and DNA_mismatch contains a specific double-stranded sequence:

5’-GGATCNNNN-3’

3’-CCTAGNNNN-5’

This sequence can be recognized by the sequence-specific nicking enzyme, Nt. Alwl, which would nick DNA_1 four nucleotides away after the GGATC sequence towards the 3’-end. Consequently, after the nicking the remaining dsDNA formed between DNA_1 and DNA_mismatch is too short to be stable, releasing the Hg^{2+} to form the next dsDNA with another DNA_1 segment on the UCNP surface.

In essence, the Hg^{2+} facilitates the nicking of DNA_1, reducing its abundance on the UCNP surface. Such hybridization and nicking process continue, resulting in potential signal amplification. Control experiments to verify the detection scheme and the nicking activity of the Nt.Alwl enzyme have been carried out, with results shown in the Supplementary Information (Supplemental Figure 2).

The detection of signal is based on LRET between $NaYF_4$: Yb^{3+}, Tm^{3+} upconversion nanoparticles and SYBR Green I. Upon excitation of a 980-nm laser, strong visible bands appear from the UCNPs at around 477, 650 and 800 nm, corresponding to the transitions from $^1G_4$, $^3F_2$, and $^3F_4$ to $^3H_6$ of Tm^{3+}, respectively. The 477-nm emission matches well

with the absorption of the SYBR Green I dye intercalated in the hairpin loop section of DNA_1 conjugated to the UCNP surface. The presence of Hg^{2+} and the subsequent nicking of DNA_1 by Nt. Alwl decrease the abundance of UCNP-DNA_1 and the number of the intercalated SYBR Green I. Consequently, the energy transfer between UCNP and SYBR Green I has been reduced, resulting in the increase of the UCNP 477-nm emission intensity. To further improve the quality of the measurement, the ratio of the 477-nm emission intensity over that of the 800-nm emission is used as the signal indicator, taking the 800-nm peak as the internal reference.

Results of the Hg^{2+} measurements are shown in Figure 4a. The limit of detection is theoretically calculated to be 0.14 nM, which is more than two orders of magnitude below the US EPA limit for mercury in drinkable water. Comparison to other published works in Table 2 show that the detection limit achieved by this method is very low. Low background signal due to the IR laser, increased quantum yield of SYBR Green when binding to dsDNA (~0.8) compared to ssDNA [37] and signal amplification assisted by Nt. Alwl are all considered to contribute to the high sensitivity. It is expected that further increase in sensitivity could be obtained by reducing the size of the UCNPs and consequently, increasing the rate of LRET.

The selectivity of this detection scheme was evaluated against some common divalent metal ions, Ba^{2+}, Cu^{2+}, Co^{2+}, and Zn^{2+}. Results shown in Figure 4b illustrate that the interference of these metal ions is negligible. Experimentally, Hg^{2+} of 0.2 nM can be detected regardless of any interference of other cations. The selectivity of the T-Hg^{2+}-T formation and the DNA sequence specificity of Nt. Alwl are the probable factors leading to the excellent selectivity of the detection of mercuric ion.

The Hg^{2+} sensing method was tested in tap water and lake water, with results summarized in Table 3. The lake water collected from Burnet Woods lake already had 2.2 nM of Hg^{2+} as measured by ICPMS. Therefore, the water sample collected from the lake was diluted with DI water before tested by this detection method. In the case of tap water, where the amount of Hg^{2+} was below the detection limit of ICPMS, a known amount of Hg^{2+} was spiked into the sample. The [Hg^{2+}] was then calculated using the linear fit equation shown in Figure 4a. In general, results from our method match reasonably well with those from ICPMS.

4. Conclusion

A novel signal amplifiable method for detection of mercuric ion is demonstrated. The method utilizes a dsDNA containing thymine mismatches as Hg^{2+} capturing element, upconversion nanoparticles as energy donor, DNA-intercalating dye as energy acceptor and sequence-specific nicking enzyme for signal amplification. This is the first report, to our knowledge, to adopt a nicking enzyme to achieve signal amplification for detection. The detecting scheme is highly sensitive to Hg^{2+} ion with good specificity and a lower detection limit of 0.14 nM, which is much lower than the US EPA limit (10 nM). The method is isothermal and can be used for detection of Hg^{2+} ions in complex matrix.

Supplementary Material

Refer to Web version on PubMed Central for supplementary material.

Acknowledgement

A.N.V. thanks Vivek Muralidharan and Rebecca N. Silva for their immense support while writing this manuscript.

REFERENCES

[1]. Cotton FA, Wilkinson G, Murillo CA, Bochmann M, Advanced Inorganic Chemistry: Sixth Edition, (1999) 1145.

[2]. Zheng N, Wang Q, Zhang X, Zheng D, Zhang Z, Zhang S. Population health risk due to dietary intake of heavy metals in the industrial area of Huludao city, China. Sci. Total Environ. 387 (2007) 96–104. doi:10.1016/j.scitotenv.2007.07.044. [PubMed: 17765948]

[3]. World Health Organisation, Mercury and Health, (n.d.) http://www.who.int/news-room/fact-sheets/detail/mercury-and-health (accessed June 18, 2018).

[4]. Tchounwou PB, Ayensu WK, Ninashvili N, Sutton D. Environmental exposure to mercury and its toxicopathologic implications for public health. Environ. Toxicol. 18 (2003) 149–175. doi:10.1002/tox.10116. [PubMed: 12740802]

[5]. Kim KH, Kabir E, Jahan SA. A review on the distribution of Hg in the environment and its human health impacts. J. Hazard. Mater. 306 (2016) 376–385. doi:10.1016/j.jhazmat.2015.11.031. [PubMed: 26826963]

[6]. Sprovieri F, Pirrone N, Ebinghaus R, Kock H, Dommergue A. Worldwide atmospheric mercury measurements : a review and synthesis of spatial and temporal trends. Atmos. Chem. Phys. Discuss. 10 (2010) 1261–1307. www.atmos-chem-phys-discuss.net/10/1261/2010.

[7]. Huang J, Su X, Li Z. Metal ion detection using functional nucleic acid and nanomaterials. Biosens. Bioelectron. 96 (2017) 127–139. doi:10.1016/j.bios.2017.04.032. [PubMed: 28478384]

[8]. Lee JS, Han MS, Mirkin CA. Colorimetric detection of mercuric ion (Hg2+) in aqueous media using DNA-functionalized gold nanoparticles. Angew. Chemie - Int. Ed. 46 (2007) 4093–4096. doi:10.1002/anie.200700269.

[9]. Jin W, Huang P, Wei G, Cao Y, Wu F. Visualization and quantification of Hg^{2+} based on anti-aggregation of label-free gold nanoparticles in the presence of 2-mercaptobenzothiazole. Sensors Actuators, B Chem. 233 (2016) 223–229. doi:10.1016/j.snb.2016.04.071.

[10]. Narayanan KB, Han SS. Highly selective and quantitative colorimetric detection of mercury(II) ions by carrageenan-functionalized Ag/AgCl nanoparticles. Carbohydr. Polym. 160 (2017) 90–96. doi:10.1016/j.carbpol.2016.12.055. [PubMed: 28115105]

[11]. Tian K, Siegel G, Tiwari A. A simple and selective colorimetric mercury (II) sensing system based on chitosan stabilized gold nanoparticles and 2,6-pyridinedicarboxylic acid. Mater. Sci. Eng. C. 71 (2017) 195–199. doi:10.1016/j.msec.2016.10.006.

[12]. Zhang Y, Zeng GM, Tang L, Chen J, Zhu Y, He XX, He Y. Electrochemical sensor based on electrodeposited graphene-Au modified electrode and nanoau carrier amplified signal strategy for attomolar mercury detection. Anal. Chem. 87 (2015) 989–996. doi:10.1021/ac503472p. [PubMed: 25440021]

[13]. Guerreiro GV, Zaitouna AJ, Lai RY. Characterization of an electrochemical mercury sensor using alternating current, cyclic, square wave and differential pulse voltammetry. Anal. Chim. Acta. 810 (2014) 79–85. doi:10.1016/j.aca.2013.12.005. [PubMed: 24439508]

[14]. Shi L, Wang Y, Ding S, Chu Z, Yin Y, Jiang D, Luo J, Jin W. A facile and green strategy for preparing newly-designed 3D graphene/gold film and its application in highly efficient electrochemical mercury assay. Biosens. Bioelectron. 89 (2017) 871–879. doi:10.1016/j.bios.2016.09.104. [PubMed: 27818041]

[15]. Zeng G, Zhang C, Huang D, Lai C, Tang L, Zhou Y, Xu P, Wang H, Qin L, Cheng M. Practical and regenerable electrochemical aptasensor based on nanoporousgold and thymine-Hg^{2+}-

thymine base pairs for Hg^{2+} detection. Biosens. Bioelectron. 90 (2017) 542–548. doi:10.1016/j.bios.2016.10.018. [PubMed: 27825522]

[16]. Tang Y, He F, Yu M, Feng F, An L, Sun H, Wang S, Li Y, Zhu D. A reversible and highly selective fluorescent sensor for mercury(II) using poly(thiophene)s that contain thymine moieties. Macromol. Rapid Commun. 27 (2006) 389–392. doi:10.1002/marc.200500837.

[17]. Bera K, Das AK, Nag M, Basak S. Development of a Rhodamine-Rhodanine-based fluorescent mercury sensor and its use to monitor real-time uptake and distribution of inorganic mercury in live zebrafish larvae. Anal. Chem. 86 (2014) 2740–2746. doi:10.1021/ac404160v. [PubMed: 24559034]

[18]. Ding SY, Dong M, Wang YW, Chen YT, Wang HZ, Su CY, Wang W. Thioether-based fluorescent covalent organic framework for selective detection and facile removal of mercury(II). J. Am. Chem. Soc. 138 (2016) 3031–3037. doi:10.1021/jacs.5b10754. [PubMed: 26878337]

[19]. Huang D, Niu C, Wang X, Lv X, Zeng G. "Turn-on" fluorescent sensor for Hg^{2+} based on single-stranded DNA functionalized Mn:CdS/ZnS quantum dots and gold nanoparticles by timegated mode. Anal. Chem. 85 (2013) 1164–1170. doi:10.1021/ac303084d. [PubMed: 23256544]

[20]. Gao ZF, Song WW, Luo HQ, Li NB. Detection of mercury ions (II) based on non-crosslinking aggregation of double-stranded DNA modified gold nanoparticles by resonance Rayleigh scattering method. Biosens. Bioelectron. 65 (2015) 360–365. doi:10.1016/j.bios.2014.10.061. [PubMed: 25461182]

[21]. Yao L, Teng J, Zhu M, Zheng L, Zhong Y, Liu G, Xue F, Chen W. MWCNTs based high sensitive lateral flow strip biosensor for rapid determination of aqueous mercury ions. Biosens. Bioelectron. 85 (2016) 331–336. doi:10.1016/j.bios.2016.05.031. [PubMed: 27183284]

[22]. Huang J, Gao X, Jia J, Kim JK, Li Z. Graphene oxide-based amplified fluorescent biosensor for Hg(2+) detection through hybridization chain reactions. Anal. Chem. 86 (2014) 3209–3215. doi:10.1021/ac500192r. [PubMed: 24564628]

[23]. US EPA. (2005). https://www.epa.gov/mercury.

[24]. Liu J, Cheng J, Zhang Y. Upconversion nanoparticle based LRET system for sensitive detection of MRSA DNA sequence. Biosens. Bioelectron. 43 (2013) 252–256. doi:10.1016/j.bios.2012.12.026. [PubMed: 23318548]

[25]. Hwang S, Im S, Sung H, Soo S, Thanh V. Upconversion nanoparticle-based Forster resonance energy transfer for detecting the IS6110 sequence of Mycobacterium tuberculosis complex in sputum. Biosens. Bioelectron. 53 (2014) 112–116. doi:10.1016/j.bios.2013.09.011. [PubMed: 24135541]

[26]. Wang P, Joshi P, Alazemi A, Zhang P. Upconversion nanoparticle-based ligase-assisted method for specific and sensitive detection of T790M mutation in epidermal growth factor receptor. Biosens. Bioelectron. 62 (2014) 120–126. doi:10.1016/j.bios.2014.06.037. [PubMed: 24995386]

[27]. Wu B, Cao Z, Zhang Q, Wang G. NIR-responsive DNA hybridization detection by high efficient FRET from 10-nm upconversion nanoparticles to SYBR green I. Sensors and Actuators B : Chemical. 255 (2018) 2853–2860. doi:10.1016/j.snb.2017.09.103.

[28]. Kuklenyik Z, Marzilli LG. Mercury(II) site-selective binding to a DNA hairpin. Relationship of sequence-dependent intra- and interstrand cross-linking to the hairpin-duplex conformational transition. Inorg. Chem. 35 (1996) 5654–5662. doi:10.1021/ic960260a. [PubMed: 11666759]

[29]. Tabata M, Sarker AK, Nyarko E. Enhanced conformational changes in DNA in the presence of mercury (II), cadmium (II) and lead (II) porphyrins. J Inorg Biochem. 94 (2003) 50–58. [PubMed: 12620673]

[30]. Ono A, Togashi H. Highly selective oligonucleotide-based sensor for mercury(II) in aqueous solutions. Angew. Chemie Int. Ed. 43 (2004) 4300–4302. doi:10.1002/anie.200454172.

[31]. Ono A. DNA-synthetic polymer conjugates. Macromol. Chem. Phys. 207 (2006) 1629–1632. doi:10.1002/macp.200600370.

[32]. Xue X, Wang F, Liu X. One-step, room temperature, colorimetric detection of mercury (Hg 2+) using DNA/nanoparticle conjugates. J. Am. Chem. Soc. 130 (2008) 3244–3245. doi:10.1021/ja076716c. [PubMed: 18293973]

[33]. Kumar M, Zhang P. Highly sensitive and selective label-free optical detection of mercuric ions using photon upconverting nanoparticles. Biosens. Bioelectron. 25 (2010) 2431–2435. doi: 10.1016/j.bios.2010.03.038. [PubMed: 20456935]

[34]. Kumar M, Zhang P. Highly sensitive and selective label-free optical detection of DNA hybridization based on photon upconverting nanoparticles. Langmuir. 25 (2009) 6024–6027. doi: 10.1021/la900936p. [PubMed: 19400568]

[35]. Dragan AI, Pavlovic R, McGivney JB, Casas-Finet JR, Bishop ES, Strouse RJ, Schenerman MA, Geddes CD. SYBR Green I: Fluorescence properties and interaction with DNA. J. Fluoresc. 22 (2012) 1189–1199. doi:10.1007/s10895-012-1059-8. [PubMed: 22534954]

[36]. Miyake Y, Togashi H, Tashiro M, Yamaguchi H, Oda S, Kudo M, Tanaka Y, Kondo Y, Sawa R, Fujimoto T, Machinami T, Ono A. Mercury(II)-mediated formation of thymine-Hg(II)-thymine base pairs in DNA duplexes. J. Am. Chem. Soc. 128 (2006) 2172–2173. doi:10.1021/ja056354d. [PubMed: 16478145]

[37]. Zipper H, Brunner H, Bernhagen J, Vitzthum F. Investigations on DNA intercalation and surface binding by SYBR Green I, its structure determination and methodological implications. Nucleic Acids Res. 32 (2004). doi:10.1093/nar/gnh101.

[38]. Liu L, Lin H. Paper-based colorimetric array test strip for selective and semiquantitative multiion analysis: Simultaneous detection of Hg^{2+}, Ag+, and Cu^{2+}. Anal. Chem. 86 (2014) 8829–8834. doi:10.1021/ac5021886. [PubMed: 25070403]

[39]. Zhang Y, Liu W, Zhang W, Yu S, Yue X, Zhu W, Zhang D, Wang Y, Wang J. DNA-mediated gold nanoparticle signal transducers for combinatorial logic operations and heavy metal ions sensing. Biosens. Bioelectron. 72 (2015) 218–224. doi: 10.1016/j.bios.2015.05.019. [PubMed: 25985196]

[40]. Zhu Z, Su Y, Li J, Li D, Zhang J, Song S, Zhao Y, Li G, Fan C. Highly sensitive electrochemical sensor for mercury(II) ions by using a mercury-specific oligonucleotide probe and gold nanoparticle-based amplification. Anal. Chem. 81 (2009) 7660–7666. doi: 10.1021/ac9010809. [PubMed: 19691296]

[41]. Zhang Y, Zuo P, Ye BC. A low-cost and simple paper-based microfluidic device for simultaneous multiplex determination of different types of chemical contaminants in food. Biosens. Bioelectron. 68 (2015) 14–19. doi:10.1016/j.bios.2014.12.042. [PubMed: 25558869]

[42]. Zuo X, Zhang H, Zhu Q, Wang W, Feng J, Chen X. A dual-color fluorescent biosensing platform based on WS_2 nanosheet for detection of Hg^{2+} and Ag+. Biosens. Bioelectron. 85 (2016) 464–470. doi:10.1016/j.bios.2016.05.044. [PubMed: 27208479]

Highlights

- Hg^{2+} detection using DNA conjugated upconversion nanoparticles with a detection limit much lower than US EPA limit of Hg^{2+} in drinking water
- Selective, sensitive and isothermal method with good reproducibility in complex matrix
- Signal amplification using nicking enzyme makes the detection scheme unique.

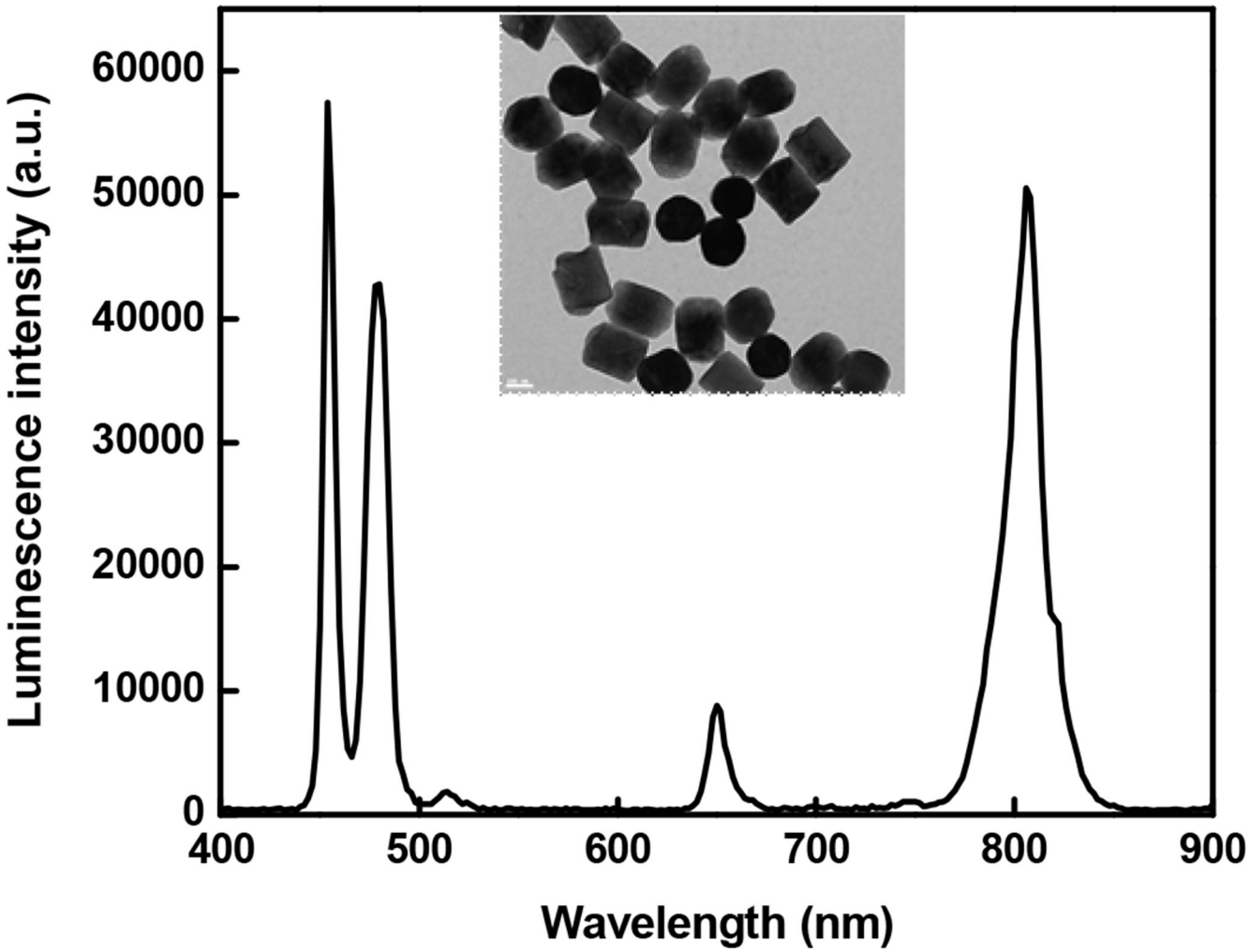

Figure 1.

TEM image and photoluminescence spectra of the synthesized $NaYF_4$: Yb^{3+}, Tm^{3+} UCNPs. Excitation wavelength is 980 nm. Scale bar in inset is 100 nm.

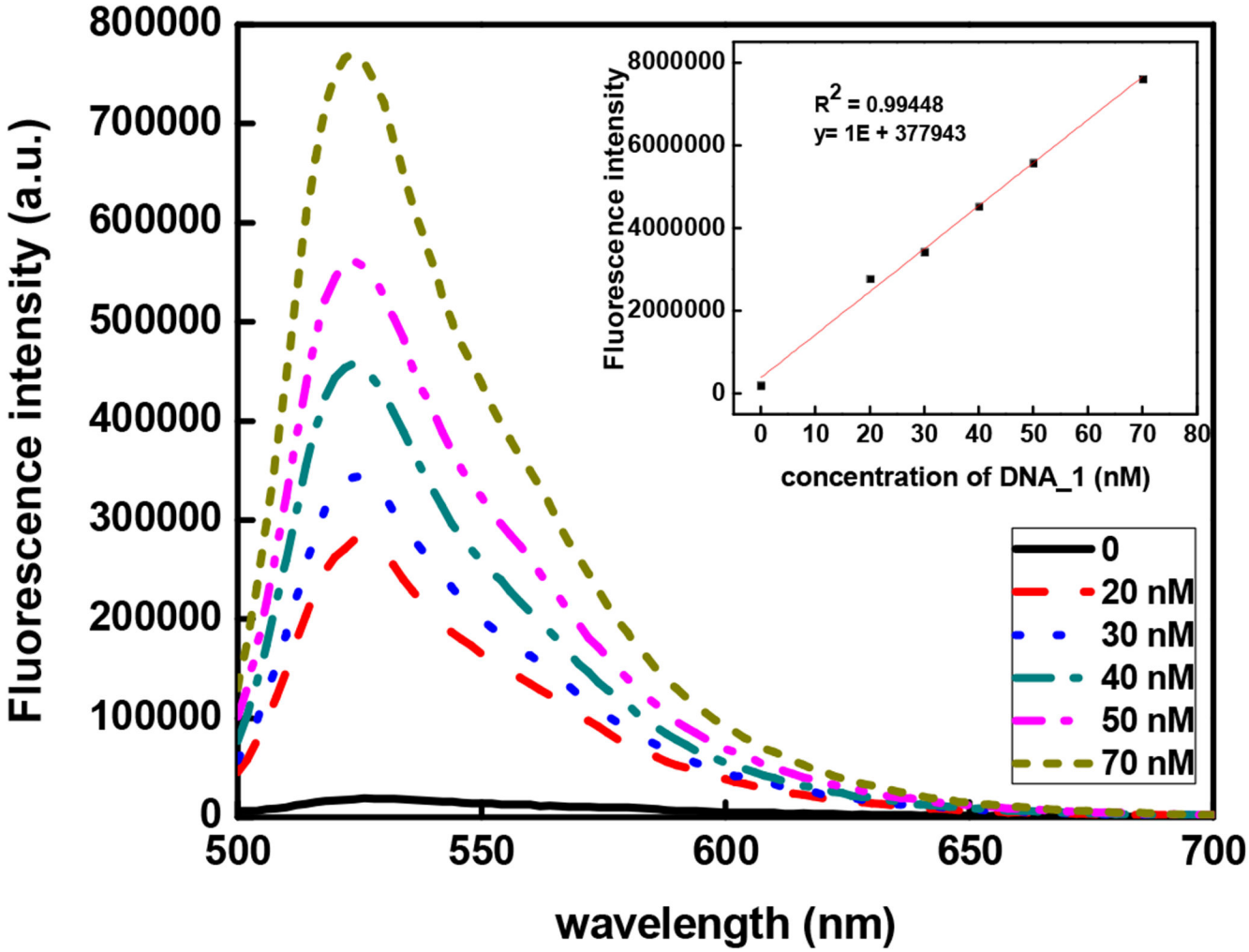

Figure 2.

SYBR Green I fluorescence emission excited at 480 nm with different concentrations of DNA_1. Calibration curve is shown in the inset.

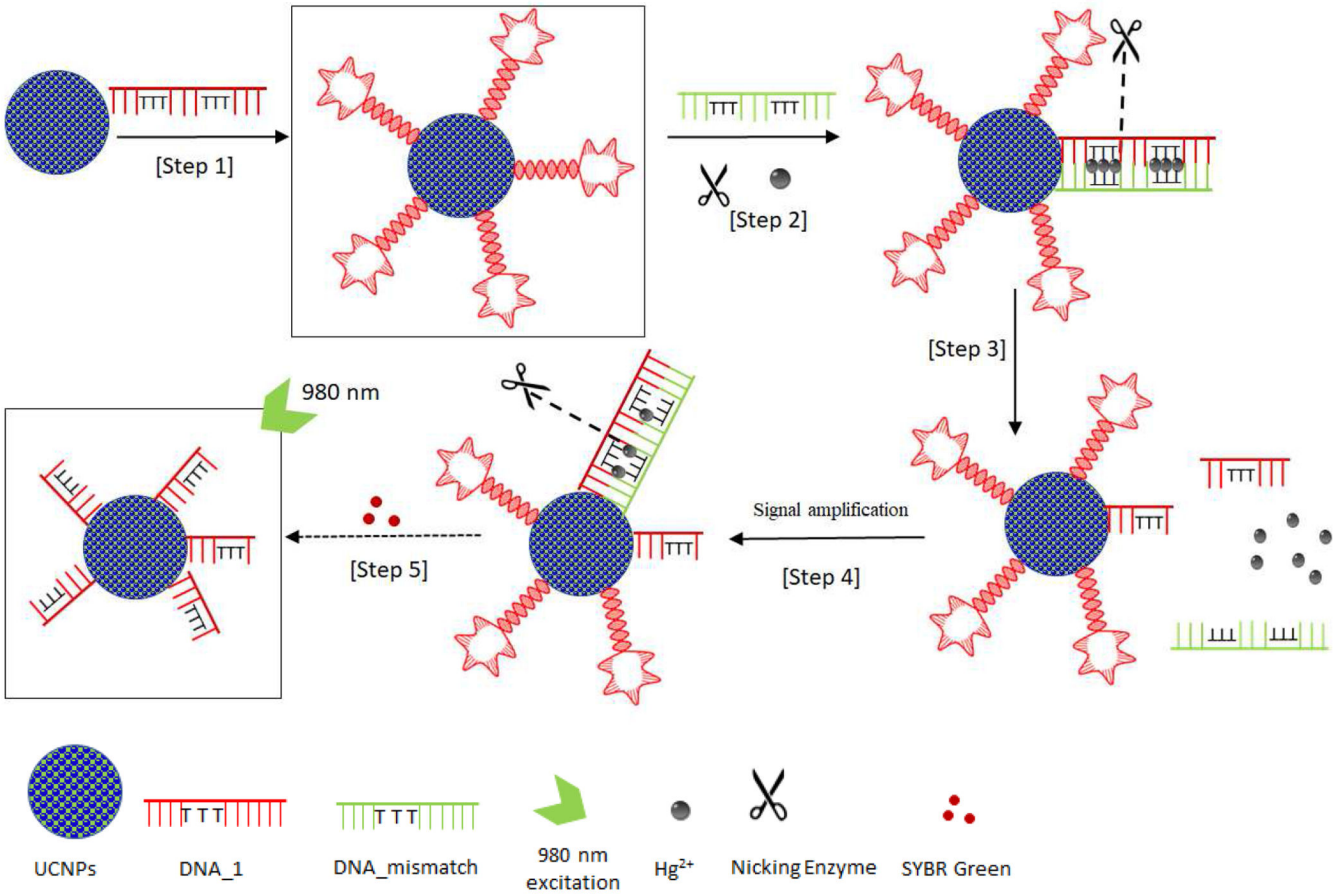

Figure 3.

Illustration of the nicking enzyme-assisted, signal-amplifiable detection of mercuric ion based on UCNPs. In the absence of Hg^{2+}, the process stops at step 2 without hybridization between DNA_1 and DNA_mismatch, and no nicking occurs.

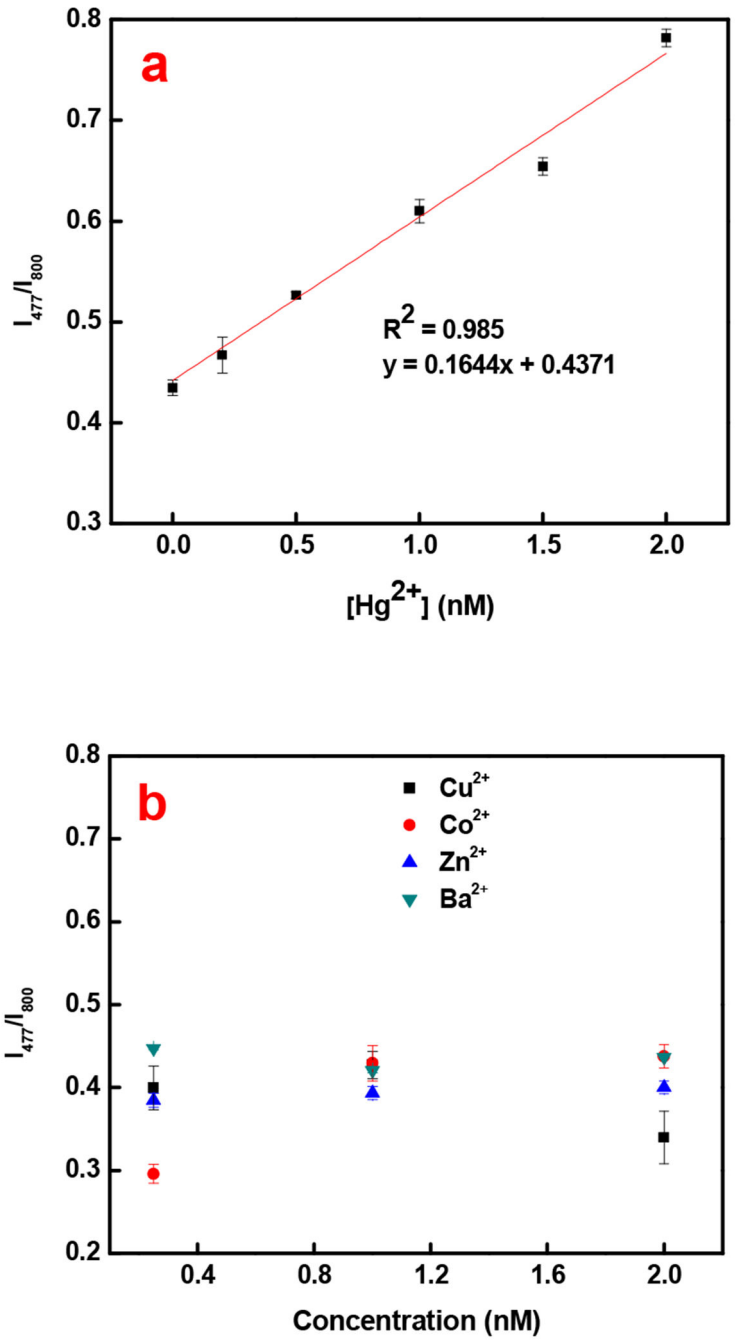

Figure 4.

a) Quantitative analysis of varying concentrations of Hg^{2+}. b) Specificity study with some common divalent cations of different concentrations.

Table 1 –

Sequence of DNA probes used in this study

DNA _1	5’-AmMC6/CATCGGATC**TTT**GC**TTT**CGATG-3’
DNA_mismatch	3’ - TCCTAG**TTT**CG**TTT**GCTAAGGA-5’

Table 2:

Comparison of limit of detection of mercuric ion

Method	Limit of detection	Reference
Colorimetric	100 nM	[8]
Colorimetric	0.19 μM	[38]
Colorimetric	2 μM	[39]
Rayleigh Scattering	0.4 nM	[20]
Electrochemical	0.5 nM	[40]
Electrochemical	10 nM	[13]
Fluorescence	121 nM	[41]
Fluorescence	3.3 nM	[42]
Fluorescence	0.3 nM	[22]
Fluorescence	0.18 nM	[19]
Upconversion	0.14 nM	This study

Table 3.

Comparison of mercuric ion detection in complex matrix

Matrix	[Hg^{2+}] determined by ICPMS	[Hg^{2+}] determined by this method
Lake water	0.51 nM±0.0016 nM	0.68±0.0019 nM
Lake water	1.25 nM±0.0038 nM	1.22±0.0054 nM
Tap water	0.50 nM±0.0016 nM	0.65±0.0031 nM
Tap water	1.38 nM±0.0042 nM	1.42±0.0054 nM